Assessing surficial foraminiferal distributions as an overwash indicator in Sur Lagoon, Sultanate of Oman

Article *in* Marine Micropaleontology · January 2011

5 authors, including:

Jessica Pilarczyk
University of Southern Mississippi

Marine Micropaleontology 80 (2011) 62–73

Contents lists available at ScienceDirect

Marine Micropaleontology

journal homepage: www.elsevier.com/locate/marmicro

Research paper

Assessing surficial foraminiferal distributions as an overwash indicator in Sur Lagoon, Sultanate of Oman

Jessica E. Pilarczyk [a,*], Eduard G. Reinhardt [a,1], Joseph I. Boyce [a,1], Henry P. Schwarcz [a,1], Simon V. Donato [a,b,1,2]

[a] School of Geography and Earth Sciences, McMaster University, 1280 Main Street West, Hamilton, Ontario, Canada, L8S 4K1
[b] Imperial Oil Resources, 237 4th Avenue Southwest, P.O. Box 2480 Station M, Calgary, Alberta, Canada T2P 3M9

ARTICLE INFO

Article history:
Received 5 July 2010
Received in revised form 31 May 2011
Accepted 3 June 2011

Keywords:
Foraminifera
Lagoon
Taphonomy
Stable isotopes
Particle-size distribution
Oman

ABSTRACT

The identification of tsunami and storm deposits in arid coastal environments can be problematic, as overwash sediments may not show significant contrasting lithologic characters with lagoonal sediments. In this study foraminifera were evaluated as an overwash indicator in a small (12 km^2) intertidal lagoon located at Sur, in the Sultanate of Oman. The lagoon is shallow (<5 m depth), tidally-controlled and communicates with the open sea through a narrow subtidal entrance channel. The lagoon is largely composed of intertidal sand and mudflats with fringing mangroves. Previous work at Sur identified evidence for overwash deposits associated with the 28 November 1945 Makran Trench tsunami (M_w 8.1) which were identified based on the presence of a laterally extensive shelly bed with distinctive taphonomic characters. In this study, particle size, stable isotopic and foraminiferal (taxa and taphonomy) analyses were conducted on surface sediment samples from Sur Lagoon to determine modern spatial trends in the lagoon for future comparison with overwash sediments deeper in the geologic record. Q-mode cluster analysis of the foraminiferal data (n = 54) found three main biofacies which follow lagoon sub-environments: Shallow Marine Area, Main Lagoon Basin, and Distal Lagoon Basin. The Shallow Marine Area is mainly subtidal with higher wave energy, the Main Lagoon Basin is predominantly intertidal with moderate wave energy, whereas the Distal Lagoon Basin is isolated and mainly intertidal with low wave energy.The most useful parameters for assessing overwash events in Sur Lagoon are the foraminifera taxa rather than the taphonomic characters themselves. The most useful taxa for recognizing an overwash (e.g. tsunami or storm) will be the abundance of *Amphistegina* spp., *Ammonia inflata*, *Elphidium advenum* and planktics which are predominantly found in the Shallow Marine Area. The abundance trend of these species with distance into the lagoon has an inverse relationship with higher r^2 values than the other taxa. Taphonomically there is a predominance of larger specimens in the Shallow Marine Area along with a higher abundance of fossil specimens.

1. Introduction

1.1. Foraminifera as an overwash indicator

After the 2004 Indian Ocean tsunami there is increased interest in the Makran Subduction Zone on the northern margin of the Arabian Sea and its potential to generate large tsunamis, but there is little geological data to assess its past history. The coastlines around the Arabian Sea may contain evidence of these past events, but they are predominantly arid and there are few tsunami indicators developed for these settings.

Foraminifera have been used as indicators of tsunami and storm overwash by documenting allochthonous tests in coastal lagoons, ponds and marshes but most of these studies have been conducted in temperate or tropical settings (e.g. Hippensteel and Martin, 2000; Scott et al., 2003; Hippensteel et al., 2005; Mamo et al., 2009 and references therein). A recent assessment of foraminifera as a tsunami indicator emphasized the importance of understanding contemporary taphonomic trends for interpreting overwash in the stratigraphic record (Mamo et al., 2009 and references therein). However, in the case of the Arabian Sea, there are few foraminiferal studies for background information and comparisons with other areas in the world may not be valid (e.g. sabkahs). Most studies from the Arabian Sea are from western India, Iran and the Persian Gulf, with few from Oman (e.g. Murray, 1965, 1966a,b,c; Reddy and Rao, 1984; El-Nakhal,

* Corresponding author. Tel.: +1 905 525 9140x27524; fax: +1 905 546 0463.
E-mail addresses: pilarcje@mcmaster.ca (J.E. Pilarczyk), ereinhar@mcmaster.ca (E.G. Reinhardt), boycej@mcmaster.ca (J.I. Boyce), schwarcz@mcmaster.ca (H.P. Schwarcz), simon.v.donato@esso.ca (S.V. Donato).
[1] Tel.: +1 905 525 9140; fax: +1 905 546 0463.
[2] Tel.: +1 403 237 2762; fax: +1 403 237 3509.

0377-8398/$ – see front matter
doi:10.1016/j.marmicro.2011.06.001

1990; Nigam and Khare, 1995; Cherif et al., 1997; Lézine et al., 2002; Bhalla et al., 2007; Moghaddasi et al., 2008; Ghosh et al., 2009). Of these studies, there are few that have examined foraminiferal distributions within lagoons (e.g. Murray, 1965, 1966a,b,c; Cherif et al., 1997).

Taphonomic evidence has been used to document paleo-environmental trends in the geological record (e.g. Parsons-Hubbard, 2005; Reinhardt et al., 2006; De Francesco and Hassan, 2008; Donato et al., 2008) and is often referred to as taphofacies analysis (Martin, 1999). Fragmentation, edge preservation, luster, encrustation, bioerosion and articulation are among the taphonomic characters often used (e.g. Martin et al., 1996; Best and Kidwell, 2000; Parsons-Hubbard, 2005; Reinhardt et al., 2006; Donato et al., 2008; Berkeley et al., 2009). The majority of the research has focussed on mollusc shells, with foraminiferal studies mostly examining vertical time averaging or lateral transport (Martin et al., 1995; Culver et al., 1996; Martin et al., 1996; Murray and Alve, 1999; Hippensteel et al., 2000). Foraminiferal provenance is a well recognized tool for determining overwash events (e.g. from open marine to lagoon) from hurricanes (e.g. Hippensteel and Martin, 1999, 2000; Scott et al., 2003; Hippensteel et al., 2005) or tsunamis (e.g. Luque et al., 2002; Hawkes et al., 2007; Kortekaas and Dawson, 2007). However, very little research has been devoted to recognizing specific taphonomic features of these event beds. Berkeley et al. (2009) document the taphonomic character of individual intertidal foraminifera, demonstrating that foraminiferal taphonomic analysis, which has been associated with information loss, can be used to provide additional information concerning depositional environment and subsequent transport histories. Recent research from Anegada, British Virgin Islands has shown foraminiferal provenance, using the ecology and taphonomy (color, fragmentation and edge rounding) of *Homotrema rubrum*, to be useful and important for assessing overwash beds in hypersaline lagoons (Pilarczyk and Reinhardt, 2011).

In this study we assess the distribution of foraminifera and their taphonomic characteristics with particle size data to determine characteristics useful for discriminating overwash deposits from lagoonal background sedimentation. These data provide baseline information for identifying and interpreting tsunami and storm overwash deposits in the stratigraphic record (Mamo et al., 2009).

1.2. Regional setting

The Sultanate of Oman has an arid, subtropical continental climatic regime. Seasonal weather changes are notably severe; in summer, temperatures peak to ~45–50 °C, whereas in winter, temperatures commonly dip to 0 °C (Lézine et al., 2002). Rainfall occurs predominantly in the winter due to eastern Mediterranean troughs which follow the Zagros Mountains and penetrate the Persian Gulf along the north of the Arabian Peninsula, with less rainfall in the summer months due to the south-western monsoon circulation (Deil, 1996). Average annual precipitation in Sur (Fig. 1) is 114.7 mm with the highest amount of precipitation falling between November and April. Humidity also peaks in the winter months (February = 70%) and drops significantly in the summer (May = 53%). Average mean monthly temperatures range from 21.7 °C in January to 34.1 °C in June (Lézine et al., 2002).

Sur Lagoon is a small (~12 km^2) tidally-dominated, micro-tidal lagoon (mean tidal amplitude ~1.2 m) situated approximately 100 km south of the capital city Muscat on the western coast of Oman (Figs. 1–2). The lagoon is divided into Distal and Main Lagoon Basins and it communicates with the Shallow Marine Area (Gulf of Oman) through a narrow (103–209 m wide) entrance channel along its eastern edge, which connects a 2.5 km network of tidal channels in the lagoon. Paleocene–Eocene aged highlands border and define most of the extent of the lagoon with the entrance channel further restricted by a low relief sand spit (~2–3 m.s.l.; Fig. 2b). Probable overwash during a storm or tsunami would follow the existing lagoon channel and possibly overtop the sand spit. Four wadi channels empty into the lagoon, the largest of which is Wadi Shamah that culminates in a ~1 km wide delta. The interior of the lagoon is made up of a series of intertidal sand and mudflats which are exposed and submerged through daily tidal cycles. At low tide ~90% of the lagoon surface is exposed, while at high tide only ~10% is exposed. Mangroves fringe most of the lagoon with the highest density along the NE tip of the Distal Basin and the SW section of the Main Basin (Fig. 2c).

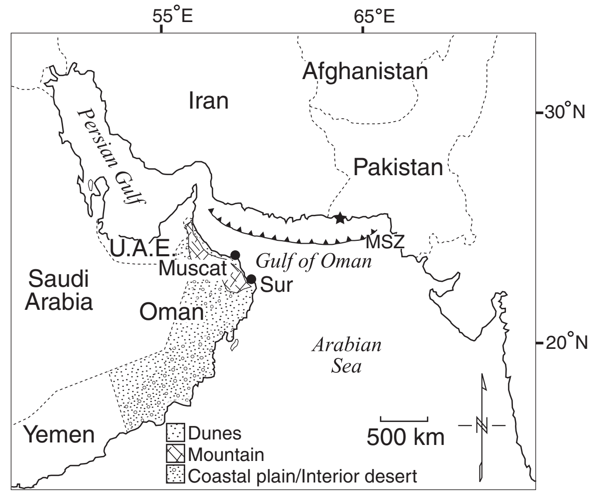

Fig. 1. Location of Sur Lagoon relative to the Makran Subduction Zone (MSZ). Epicentre of the 28 November 1945 tsunamigenic earthquake (M_w 8.1; black star) and broad-scale geologic features within Oman indicated.

The Shallow Marine Area outside of the lagoon has a narrow shelf which drops off to depths of over 200 m after ~5 km (Szuman et al., 2006). The coastline of north-eastern Oman supplies continuous sediment to the Gulf of Oman through erosion of prominent rocky headlands and ephemeral wadis. Wave action in the nearshore environment is high due to the large fetch associated with the Gulf of Oman. In contrast, the restricted lagoon basins experience little wave action and are predominantly tidal. Wadi systems (e.g. Wadi Shamah) provide poorly sorted sediment (muds–gravels) to the lagoon; whereas, predominantly fine to medium sands come from the Gulf of Oman.

Field observations and a Digital Elevation Model (DEM) were used to determine 12 sub-environments (Donato et al., 2008, 2009; Fig. 2c). These include: wadi, mangrove area, mudflat, lagoon shoreface, sandflat, lagoon creek (intertidal), flood delta, shelly firm ground, lagoon channel (subtidal), wadi delta, entrance channel and marine shoreface (Fig. 2c).

1.3. Overwash evidence in Sur Lagoon

Previous research from Sur Lagoon focused on the identification and characterization of a tsunami deposit from the 28 November 1945 Makran Trench earthquake (Donato et al., 2008, 2009). The seismically active Makran Subduction Zone (MSZ) located off the coast of Pakistan has been known to produce tsunamigenic earthquakes that have impacted the coasts of Iran, Pakistan, India and Oman (e.g. Heidarzadeh et al., 2008; Okal and Synolakis, 2008). Little is known about the MSZ, and predictions of future events are based on historical information as no geologic (i.e. tsunami deposit) evidence has been available (Ambraseys and Melville, 1982). Donato et al. (2008) documented an event horizon in Sur Lagoon, Oman inferred to be from the 1945 Makran Trench event, which consisted of a coarse shell-rich layer with distinctive taphonomic characteristics and

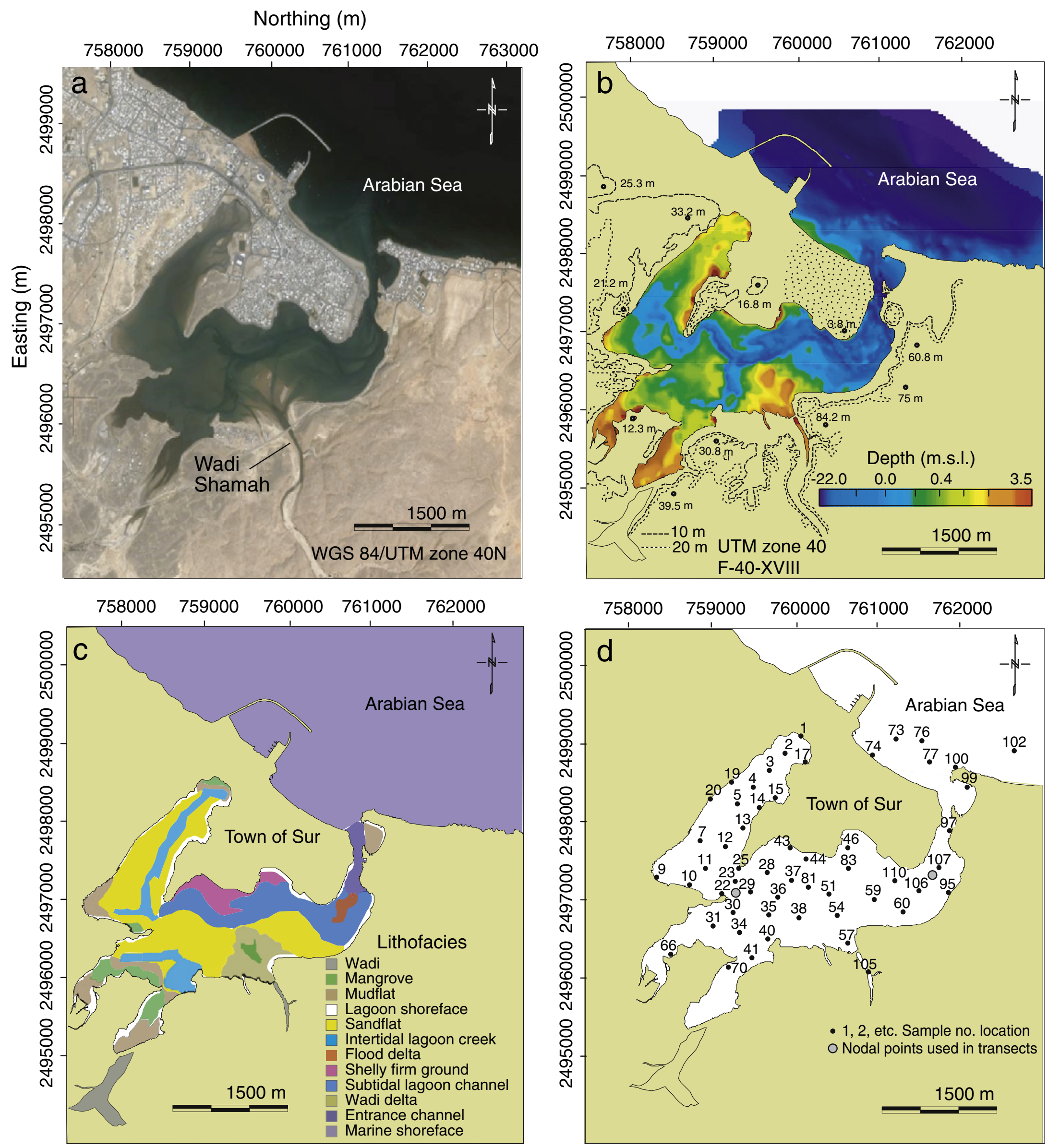

Fig. 2. a) Satellite image of Sur Lagoon obtained from Google Earth. b) Digital Elevation Model (DEM) of the study area using data collected with a Trimble R3 unit and a Lowrance SONAR. c) Sedimentary sub-environments within the lagoon. Colors correspond to varying lithofacies identified during a field survey, DEM analysis, and satellite imagery. d) Location of surface samples used in the foraminiferal analysis. Nodes at the base of the entrance channel and at the Main–Distal Lagoon boundary were used to calculate the distance of each sample location relative to the marine source (Figs. 7–9).

particle size trends: thick (5–25 cm), laterally extensive (>1 km^2), sheet-like geometry that thinned and became finer grained with distance inland from the lagoon entrance, and contained whole and fragmented lower-shore offshore bivalves (Donato et al., 2008, 2009).

Cyclone activity in the northern Arabian Sea is rare and is generally characterized by small cells that dissipate quickly. However, the recent cyclones Gonu (Category 5; 2007) and Phet (Category 3; 2010) are considered exceptional and represent the most 'severe cyclonic storms' to strike the Arabian Peninsula in recorded history (Fritz et al., 2010). At Ras al-Hadd which is approximately 30 km east of Sur, Fritz et al. (2010) reported a 5 m high storm surge and a 200 m landward incursion of seawater. A field survey at Sur in November 2007 showed that Gonu's rain (>610 mm) and resulting flow through Wadi Shamah eroded the small delta and washed away the bridge (Donato et al., 2009). Despite the estimated storm surge of 2.6 m, surveys of the lagoon after the event found no record of overwash or shells (Donato et al., 2009). Most of the sediment moved seaward into the Shallow Marine Area bypassing the Main Lagoon Basin, although lesser events would likely contribute sediment directly to the lagoon.

2. Materials and methods

In March 2006 (i.e. before Gonu), 111 sediment samples (upper 2 cm) were collected along 12 transect lines spaced ~300 m apart (Fig. 3). Sample locations used in the microfossil analysis are shown in

Fig. 3. Particle-size distribution (PSD) plots for Sur Lagoon based on percent abundance of particle size fraction (0–11 Φ). Sample locations (n = 111) used for particle-size analysis are represented by black circles.

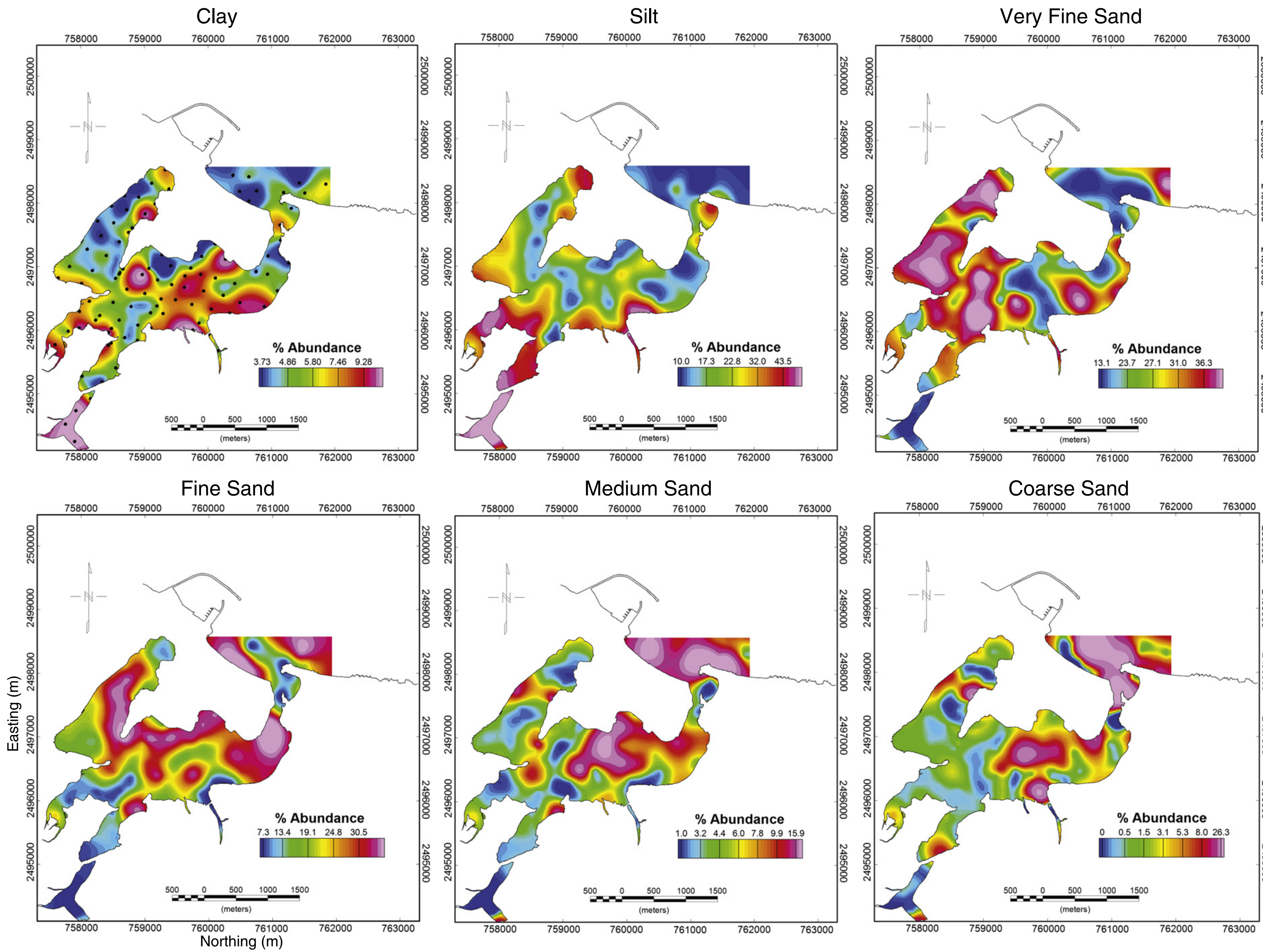
Clay
% Abundance
3.73 4.86 5.80 7.46 9.28
Silt
% Abundance
10.0 17.3 22.8 32.0 43.5
Very Fine Sand
% Abundance
13.1 23.7 27.1 31.0 36.3
Fine Sand
% Abundance
7.3 13.4 19.1 24.8 30.5
Medium Sand
% Abundance
1.0 3.2 4.4 6.0 7.8 9.9 15.9
Coarse Sand
% Abundance
0 0.5 1.5 3.1 5.3 8.0 26.3
500 0 500 1000 1500
(meters)
758000 759000 760000 761000 762000 763000
2495000 2496000 2497000 2498000 2499000 2500000
Easting (m)
Northing (m)

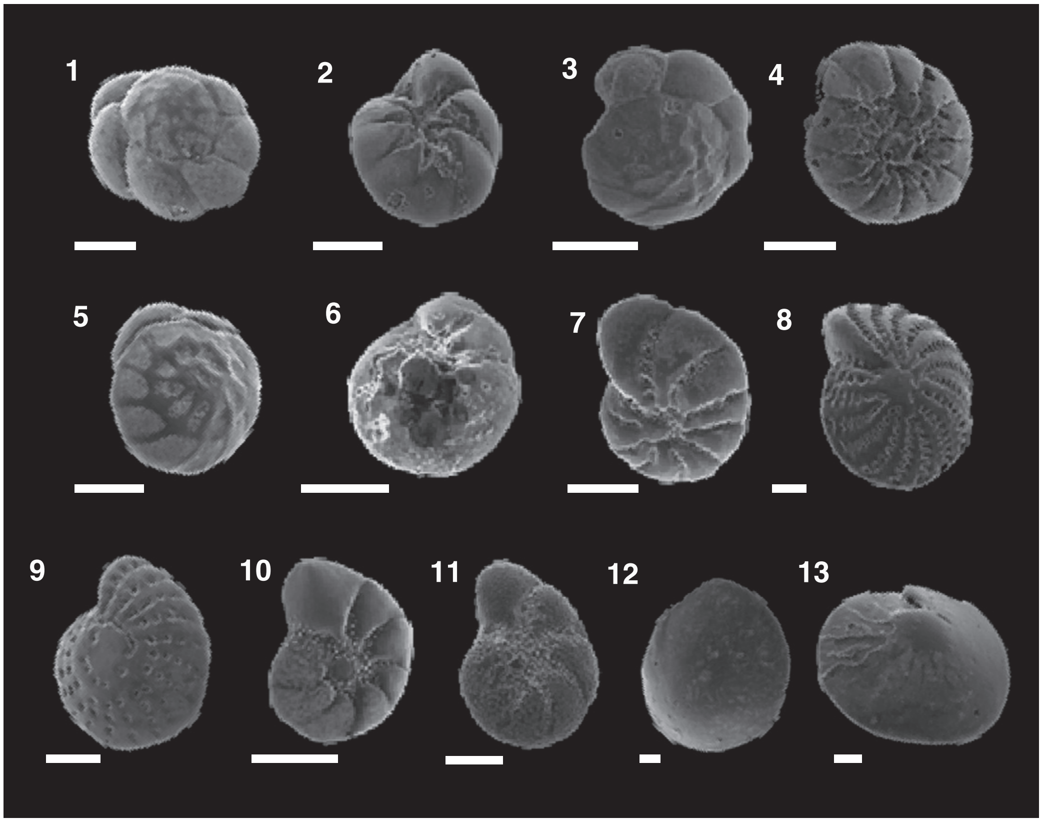

Plate 1. All scale bars are equal to 100 μm. 1. *Ammonia tepida* ventral view. 2. *Ammonia tepida* dorsal view. 3. *Ammonia parkinsoniana* ventral view. 4. *Ammonia parkinsoniana* dorsal view. 5. *Ammonia inflata* ventral view. 6. *Ammonia inflata* dorsal view. 7. *Elphidium gerthi* side view. 8. *Elphidium craticulatum* side view. 9. *Elphidium striatopunctatum* side view. 10. *Elphidium advenum* side view. 11. *Porosononion granosa* side view. 12. *Amphistegina lessonii* ventral view. 13. *Amphistegina lobifera* ventral view.

Fig. 2d. Nearshore marine samples were collected by free-diving along similar grid lines. All sub-environments within the lagoon and marine embayment were sampled (e.g. entrance channel, intertidal, subtidal, mangrove area, sandflat, mudflat, beach, shallow marine, wadi).

A Trimble differential GPS (D-GPS) unit was used to create a digital elevation model of the modern lagoon surface (DEM; Fig. 2b; Donato et al., 2009). The DEM was produced by walking the D-GPS in north–south transects spaced 100 m apart, and east–west lines at 300 m spacing. A single-beam echo sounder was used to survey depths greater than 1.5 m within the lagoon, the entrance channel, and the Shallow Marine Area ~1 km out from the coastline. Both datasets were combined using Geosoft Oasis TM software to create the DEM and were leveled to a mean sea level datum (see Donato et al., 2008).

2.1. Foraminiferal analysis

Samples (n = 54) were selected for foraminiferal analysis based on the facies and spatial distribution within the lagoon (Fig. 2c; Online Table S1). Fifty-five samples were collected; however, only 54 were used for foraminiferal analysis. Due to limited sample volume, geochemical analysis required the use of an additional sample (sample no. 35), which is indicated in Fig. 2d. Samples ranged in volume from 5 to 20 cm^3 and were sieved (>63 μm), dried, randomly split to provide specimen counts of ~300, and analyzed using an Olympus SZX12® microscope. A total of 22 foraminifera taxa (Plate 1; Table 1; Online Table S2) were identified using the taxonomy of Hottinger et al. (1993) and Hayward et al. (2004). Scanning Electron Microscopy (SEM) was conducted at the Brockhouse Institute for Materials Research at McMaster University (Plates 1–2).

Q-mode (statistically similar populations) and R-mode (statistically affiliated populations) cluster analysis of the foraminiferal data (% species) was performed in the statistical software package PAST™ (Fig. 4). Q-mode cluster analysis used Ward's Minimum variance and is reported as squared Euclidean distances (Fishbein and Patterson, 1993). Standard error was calculated on the fractional abundances following Patterson and Fishbein (1989) and species that had standard errors greater than relative fractional abundances in all samples were eliminated from the cluster analysis. A total of 16 species were found to be statistically significant in at least one sample: *Ammonia inflata*, *Ammonia parkinsoniana*, *Ammonia tepida*, *Amphistegina* spp., *Patellinella* sp., *Brizalina striatula*, *Cibicides pseudolobatulus*, *Elphidium advenum*, *Elphidium craticulatum*, *Elphidium gerthi*, *Elphidium striatopunctatum*, *Peneroplis planatus*, *Porosononion granosa*, *Rosalina orientalis*, miliolids and planktics (Fig. 4; Table 1; Online Table S2). *Amphistegina lessonii* and *Amphistegina lobifera* were combined as were *Cycloforina carinata*, *Pseudotriloculina laevigata*, *Quinqueloculina multimarginata*, *Quinqueloculina patagonica* and *Quinqueloculina seminulum* as they share similar ecological constraints and combining them produced better cluster results (Fig. 4).

Taphonomic analysis used the following characters: (1) unaltered, (2) degree of fragmentation (small fragment: <49% of specimen, large fragment: >50% of specimen), (3) degree of corrasion (combined influence of corrosion and abrasion; minimal, moderate, maximal), and (4) size (>500 μm, 250–500 μm, 150–250 μm, <150 μm). In addition, the abundance of in-filled fossil specimens was recorded although, they were heavily altered and could not be reliably identified to the species level (Fig. 5; Plate 2; Table 2; Online Table S3). This taphonomic data was clustered using the same method as described previously (Fig. 6).

Plots of taxa and taphonomic characters vs. linear distance into lagoon used measurement nodes in the entrance channel (0 km) and at the transition (2.5 km) between the Distal and Main Lagoon Basins

Table 1
Biofacies elevation, exposure time, average Shannon Diversity Index (SDI) and foraminiferal abundances (mean% ± 1 std.) for the three biofacies determined with cluster analysis.

Biofacies	BF_A	BF_B	BF_C
Elevation (m.s.l.)	0.6 ± 0.5	0.3 ± 0.6	−0.8 ± 1.1
Exposure time (h/day)	11	8	0
Shannon–Weaver Diversity (SDI)	1.8 ± 0.1	1.9 ± 0.1	2.0 ± 0.2
Ammonia inflata	0	<1	2 ± 2
Ammonia parkinsoniana	14 ± 5	17 ± 5	18 ± 7
Ammonia tepida	13 ± 5	12 ± 7	6 ± 11
Amphistegina spp.	<1	2 ± 2	12 ± 13
Patellinella sp.	<1	<1	5 ± 7
Brizalina striatula	4 ± 2	3 ± 1	1 ± 1
Cibicides pseudolobatulus	1 ± 2	1 ± 2	1 ± 2
Elphidium gerthi	11 ± 6	15 ± 6	10 ± 6
Elphidium craticulatum	2 ± 2	2 ± 2	2 ± 2
Elphidium advenum	<1	<1	2 ± 2
Peneroplis planatus	9 ± 5	7 ± 4	2 ± 3
Elphidium striatopunctatum	2 ± 2	2 ± 4	<1
Porosononion granosa	4 ± 2	3 ± 3	2 ± 2
Miliolids	37 ± 8	28 ± 10	22 ± 12
Planktics	2 ± 2	6 ± 3	14 ± 10

(Fig. 2d). Nodal points were taken from Donato et al. (2009) where, in order to investigate spatial changes in the 1945 tsunami bed at Sur Lagoon, several nodal points were plotted within the lagoon. Distances (line of sight) from the nodal point were measured in a westerly direction for points in the lagoon while samples outside the lagoon have negative distances and were measured in a N–NW direction. These measurement nodes were selected to reflect a probable transport path for a marine incursion (storm or tsunami; Figs. 7–9).

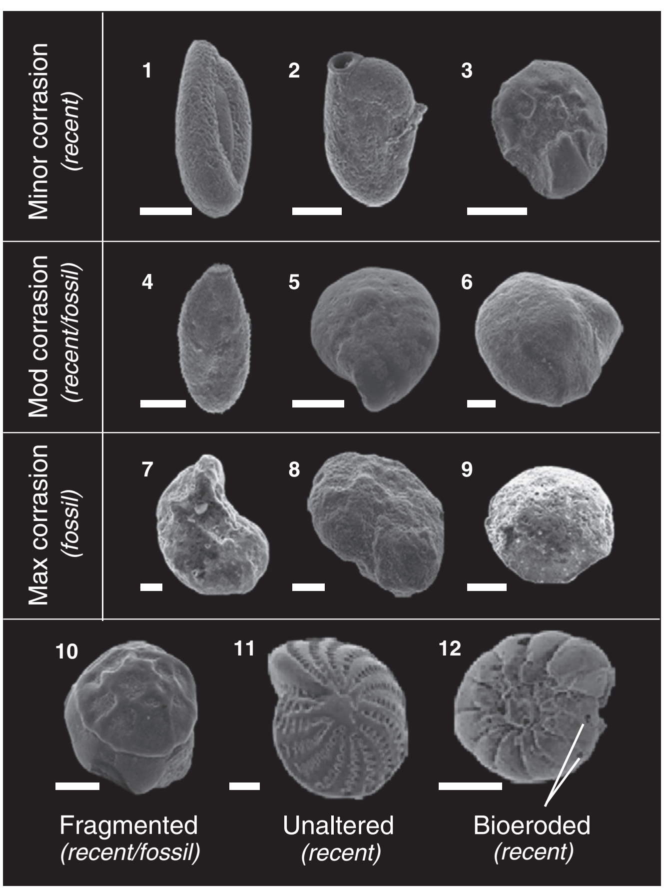

Plate 2. All scale bars represent 100 μm. 1–3. Minimally corraded recent individuals (recent only). 4–6. Moderately corraded individuals (recent and fossil). 7–9. Maximally corraded fossil individuals (fossil only). 10. Fragmented individual (recent and fossil). 11. Taphonomically unaltered individual (recent only). 12. Bioeroded individual (recent only).

2.2. Stable isotopic analysis

Unaltered *A. parkinsoniana* specimens (n = 3 to 5; 85–100 μg) were selected for stable isotopic analysis ($\delta^{18}O$, $\delta^{13}C$) from 22 of the surface samples obtained along a transect within the lagoon. *A. parkinsoniana* was chosen due to its abundance in all samples and because it has been reported to have minimal microhabitat effects (Chandler et al., 1996). Prior to analysis, samples were washed in an ultrasonic bath of distilled water to remove any sediment particles. SEM analysis showed that the selected specimens were free from any encrustation or sediment in-filling. Stable isotopic analysis was performed on the Finnigan Delta Plus XP® mass spectrometer ($\delta^{13}C$ precision = ± 0.10; $\delta^{18}O$ precision = ± 0.07) at McMaster University's Stable Isotope Research Laboratory (MSIRL). Values are reported relative to VPDB and are the average of two trials for each sample location.

2.3. Particle size analysis

Sediment samples (n = 110) were treated with 10% HCl to remove carbonates (54 ± 7% removed) and 40% H_2O_2 to remove organic material (<1% removed). The remaining siliciclastic fraction was sieved using an 1800 μm mesh before analysis with a Beckman Coulter LS 230 laser diffraction particle size analyzer. Samples were stirred as a moist paste to homogenize the sediment, then ultrasonically disaggregated with hexametaphosphate $(NaPO_3)_6$ to reduce flocculation. Particle size values were calculated using the Fraunhofer Optical Model (Murray, 2002; van Hengstum et al., 2007; Online Table S1) and are the average of two replicates. Particle sizes were converted to the Wentworth Phi Scale, interpolated and gridded using a Triangular Irregular Network (TIN) algorithm according to Sambridge et al. (1995), and plotted as Particle Size Distribution (PSD) plots in Geosoft Oasis TM (Fig. 3).

3. Results

3.1. Bio- and taphofacies

R-mode cluster analysis shows that populations of *A. tepida*, *A. parkinsoniana*, *E. gerthi*, *P. planatus* and miliolids are closely associated and are predominantly found in the lagoon basins (Distal and Main); whereas *A. inflata*, *Amphistegina* spp., *Patellinella hanzawai*, *B. striatula*, *C. pseudolobatulus*, *E. advenum*, E. *craticulatum*, *E. striatopunctatum*, *P. granosa*, *R. orientalis*, and planktics are mostly found in the Shallow Marine Area. Q-mode cluster analysis of taxonomic and taphonomic data produced dendrograms with three biofacies and taphofacies: Biofacies A (BF_A), BF_B and BF_C; Taphofacies A (TF_A), TF_B and TF_C (Figs. 4 and 5). Generally, biofacies correspond well with lagoon areas although inter-sample variabilities were quite high with high standard-deviations (Fig. 6).

3.1.1. Distal Lagoon Basin (BF_A, TF_A)

BF_A is predominantly found in the Distal Lagoon Basin located in the westernmost arm of the lagoon (Fig. 6a), which has the highest mean elevation (n = 17; E_{avg} = 0.6 ± 0.5 m.s.l.) and the most subaerial exposure time over tidal cycles (e_x = 11 h/day; Table 1). BF_A is characterized by high proportions of miliolids (37 ± 8%), *A. parkinsoniana* (14 ± 5%), *A. tepida* (13 ± 5%), *E. gerthi* (11 ± 6%) and *P. planatus* (9 ± 5%), with a near absence of open marine benthics including *A. inflata*, *Amphistegina* spp. and planktics (<2%). Main Lagoon Basin samples 44 and 28 cluster with BF_A probably because their elevations were relatively high for this

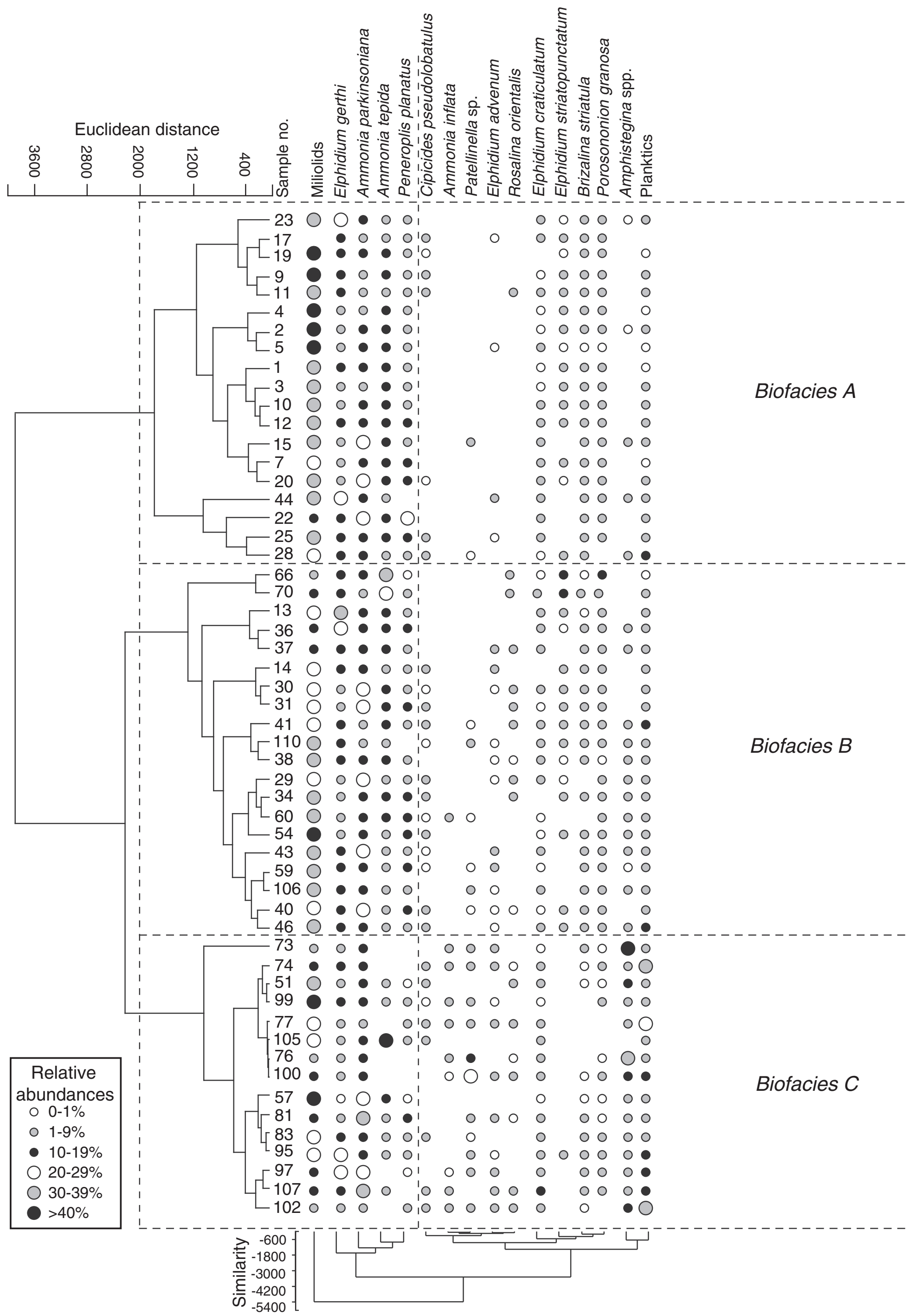

Fig. 4. Q-mode vs. R-mode cluster analysis using Ward's method indicating three biofacies.

part of the basin. Mean Shannon Diversity Index (SDI) values at 1.8 ± 0.1 (Table 1) indicate that the Distal Lagoon Basin is a transitional (SDI = 1.5–2.5) environment rather than stable (SDI = 2.5–3.5) or stressed (SDI = 0.1–1.5; e.g. Patterson and Kumar, 2000, 2002). In fact, all sample locations within the lagoon exhibited SDIs within the transitional range (1.5–2.4), except sample 57 (SDI = 1.4) which reflects a stressed environment at the mouth of Wadi Shamah (Fig. 8; Table 1). Generally, the diversity decreases with increased tidal exposure time (Shallow Marine Area = 2.0 ± 0.2; Main Lagoon Basin = 1.9 ± 0.1; Distal Lagoon Basin = 1.8 ± 0.1; Table 1), although there is considerable overlap in these values. It is questionable as to whether the SDIs are a true reflection of conditions within the lagoon as transport of allochthonous tests is likely to be quite high.

The Distal Lagoon Basin is predominantly made up of TF_A (n = 16; Fig. 6b; Table 2). The TF_A has the highest abundance of recent relative to fossil specimens (84 ± 8%), as well as the most unaltered recent foraminifera (51 ± 22%) with the highest values of corrasion (31 ± 14%) and bioerosion (11 ± 7%). Fossil specimens are low in abundance (16 ± 8%) and did not seem to have any distinctive characteristics (Table 2).

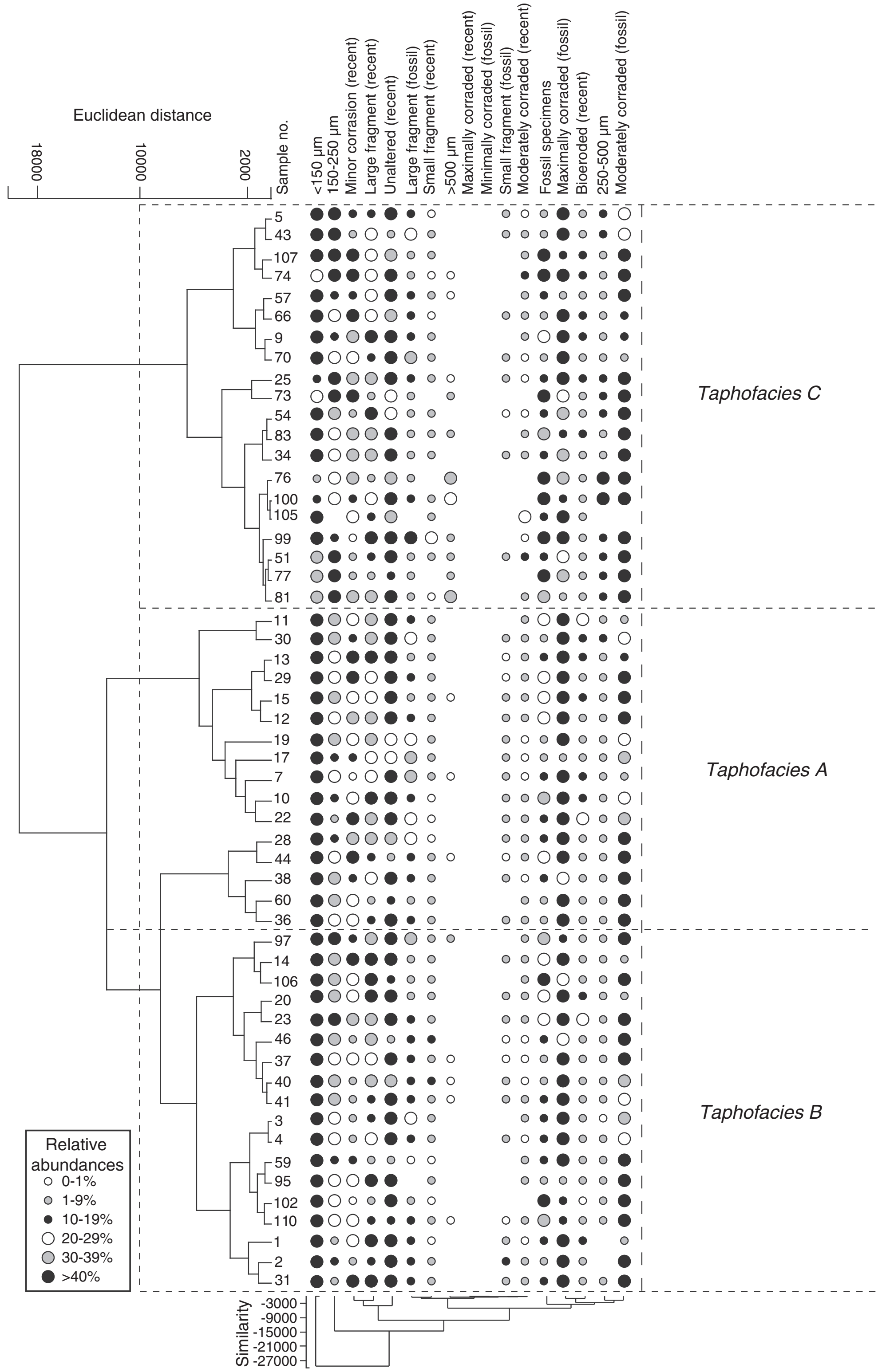

Fig. 5. Q-mode vs. R-mode cluster analysis using Ward's method indicating three taphofacies.

3.1.2. Main Lagoon Basin (BF_B, TF_B)

Biofacies B (n = 20) is predominantly found in the Main Lagoon Basin with a mean elevation and tidal exposure time slightly lower than that of the Distal Lagoon ($E_{avg} = 0.3 \pm 0.6$ m.s.l., $e_x = 8$ h/day; Table 1; Fig. 6a). There are only minor differences in the biofacies composition relative to BF_A. Miliolids (28 ± 10%), *A. parkinsoniana* (17 ± 5%), *E. gerthi* (15 ± 6%) and *A. tepida* (12 ± 7%) are still the dominant taxa; however, the presence of minor allochthonous species (planktics: 6 ± 3%; *Amphistegina* spp.: 2 ± 2%; and *A. inflata:* <1%) distinguishes it from BF_A in the cluster analysis (Fig. 4; Table 1). The network of intertidal channels connecting the Main Lagoon Basin with the Shallow Marine Area is the likely source for these taxa which would be transported into the lagoon via storms and tidal currents (e.g. *Amphistegina* spp. = 12 ± 13%). These taxa are virtually absent in the Distal Lagoon Basin (Table 1).

Table 2
Taphofacies elevation, exposure time, and average foraminiferal taphonomic characteristics (mean% ± 1 std.) for the three taphofacies determined with cluster analysis.

Taphofacies	TF_A	TF_B	TF_C
Taphofacies elevation (m.s.l.)	0.4 ± 0.3	0.2 ± 1.1	−0.1 ± 1.4
Exposure time (h/day)	11	8	0
Specimen size			
>500 μm	<1	<1	4 ± 8
250–500 μm	6 ± 3	4 ± 3	13 ± 12
150–250 μm	27 ± 9	26 ± 10	35 ± 17
<150 μm	67 ± 11	69 ± 13	48 ± 25
Recent foraminifera			
Total recent	84 ± 8	78 ± 14	68 ± 25
Minor corrasion	29 ± 13	21 ± 19	25 ± 17
Moderate corrasion	2 ± 1	2 ± 2	4 ± 6
Maximal corrasion	0	0	0
Total corrasion	31 ± 14	22 ± 19	29 ± 19
Small fragment	3 ± 2	4 ± 5	3 ± 5
Large fragment	29 ± 10	28 ± 15	26 ± 18
Total fragments	32 ± 10	32 ± 17	30 ± 23
Bioeroded	11 ± 7	6 ± 6	7 ± 4
Unaltered	51 ± 22	45 ± 28	49 ± 21
Fossil foraminifera			
Total fossil	16 ± 8	22 ± 14	32 ± 25
Minor corrasion	0	0	0
Moderate corrasion	34 ± 20	49 ± 29	56 ± 31
Maximal corrasion	66 ± 20	51 ± 29	45 ± 31
Small fragment	2 ± 1	3 ± 5	1 ± 2
Large fragment	17 ± 9	11 ± 6	10 ± 8
Total fragments	19 ± 9	14 ± 10	12 ± 10

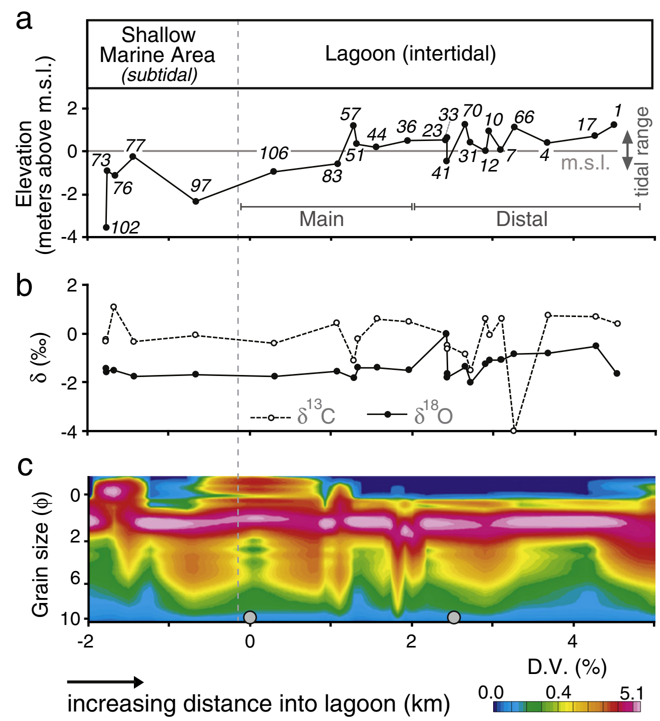

Fig. 7. a) Elevation along a transect from the Shallow Marine Area through the Main and Distal Lagoon Basins using nodes shown in Fig. 2d. b) Stable isotope data for sample locations along the transect. c) Particle-size plots for the transect (D.V.% = differential volume percent).

TF_B is predominantly made up of recent specimens (78 ± 14%) which is slightly lower than TF_A (84 ± 8%), but higher than TF_C (68 ± 25%; Table 2; Fig. 6b). The other taphonomic characters are very similar to those in TF_A with only minor differences (e.g. corrasion and bioerosion; Table 2) although, there are larger differences with the Shallow Marine Area.

3.1.3. Shallow Marine Area (BF_C, TF_C)

Biofacies C (n = 15) is mainly found in the Shallow Marine Area, embayment and also subtidal regions of the lagoon and has the lowest elevations (−0.8 ± 1.1 m.s.l; i.e. open marine, entrance channel, main subtidal channel; Table 1; Fig. 6a). BF_C is characterized by lower abundances of miliolids (22 ± 12%) and *A. tepida* (6 ± 11%), and higher abundances of planktics (14 ± 10%), *Amphistegina* spp. (12 ± 13%), *Patellinella* sp., (5 ± 7%) and *A. inflata* (2 ± 2%). *A. inflata* abundances are low but important, as it is absent to very low in the lagoon basins. In general, the largest and most robust species (e.g.

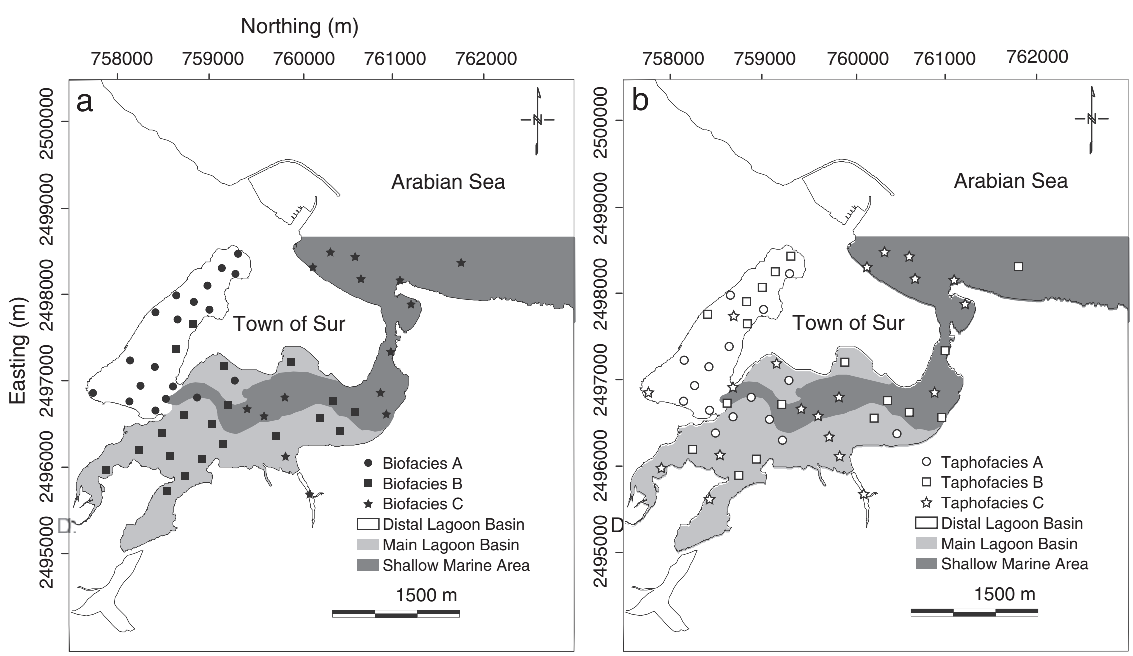

Fig. 6. Distribution of biofacies (a) and taphofacies (b) showing relationship with geographic boundaries (Distal Lagoon Basin, Main Lagoon Basin and Shallow Marine Area).

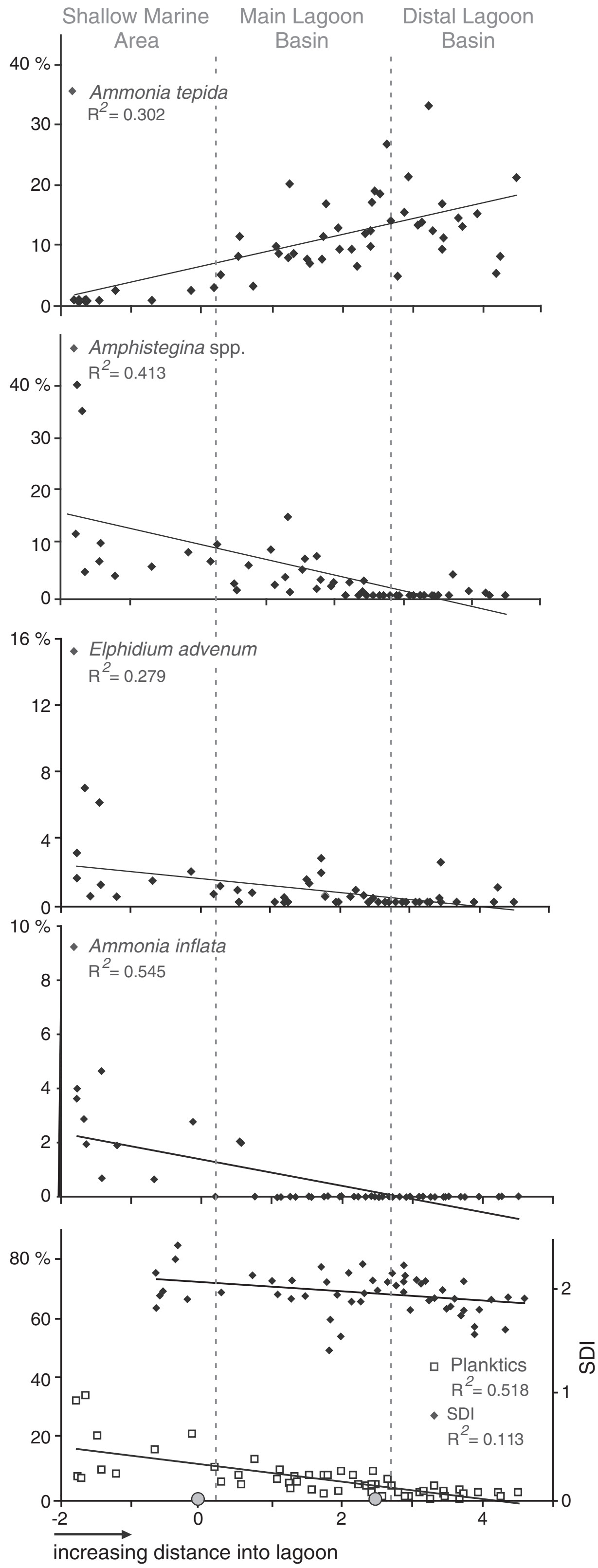

Fig. 8. Abundances of significant taxa and Shannon–Weaver Diversity Index (SDI) vs. distance from the Shallow Marine Area outside the lagoon using nodes shown in Fig. 2d.

Amphistegina spp.) tend to dominate the Shallow Marine Area which has higher wave and current energies. The taphonomic characters show similar trends with high abundances of robust fossil specimens

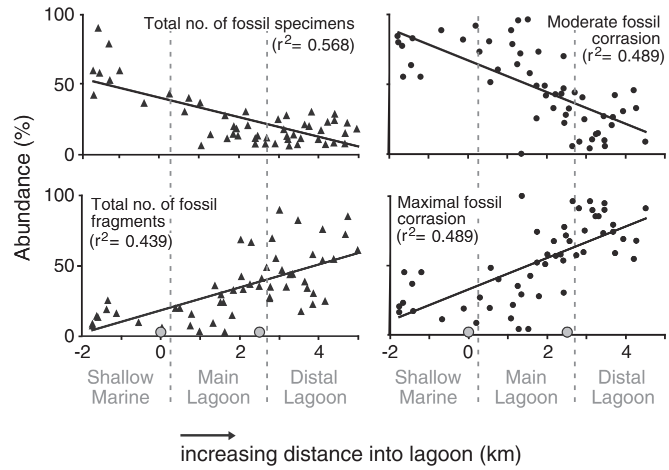

Fig. 9. Dominant taphonomic characters vs. distance from the Shallow Marine Area outside the lagoon using nodes shown in Fig. 2d.

(32 ± 25%), and large sized foraminifera (>500 μm = 4 ± 8%; 250–500 μm = 13 ± 12%), compared to the Distal and Main Lagoon Basins (Tables 1–2; Peebles and Lewis, 1991).

3.2. Stable isotopes

The stable isotopic data shows minor variations and is not useful in distinguishing subenvironments (Fig. 7). Generally, the subtidal Shallow Marine Area and the Main Lagoon Basin have slightly more negative δ^{18}O values ($\delta^{18}O_{avg} = -1.7 \pm 0.1$‰) than the intertidal environments in the Distal Lagoon Basin ($\delta^{18}O_{avg} = -1.3 \pm 0.4$‰). This lack of contrast seems unusual since the intertidal areas would have higher average temperatures and evaporation rates with the 8–10 h/day subaerial exposure (Fig. 7). The Gulf of Oman off Sur has sea surface temperatures of ~27 °C and salinities of ~36.5 ppt (Sultan and Elghribi, 1996; Schils and Wilson, 2006). Measured salinity and temperature in the mangrove areas are higher (41.7–44.2 ppt; 26–29 °C) than the open sea, so some evaporative effect would be expected. The lack of contrast in values maybe due to taphonomic biases resulting from the reworking of older tests, or the transport of specimens from subtidal areas of the lagoon.

Similarly the δ^{13}C values follow no trend and are more variable within the lagoon, likely due to the taphonomic issues already pointed out, but also due to the complexity of factors affecting the dissolved inorganic carbon of the water (e.g. salinity, productivity and OM decomposition; Mackensen et al., 2001; Bickert and Mackensen, 2004; Peros et al., 2007).

3.3. Particle size

Generally, the fine silt and clay sized sediment is found in the mangrove areas on the southern lagoon margin as well as the Wadi Shamah deltaic area. Sandy sediments dominate the rest of the Lagoon (Main and Distal) and Shallow Marine Area. The Shallow Marine Area tends to have very coarse sand which transitions to medium sand in the Main Lagoon and fine to very fine sand in the Distal Lagoon (Fig. 3). The PSD transect with increasing penetration distance into the lagoon (Fig. 7), shows a coarse PSD tail (0 phi) in the Main Lagoon Basin but not in the Distal Lagoon Basin. This transition from coarse to fine particle sizes separates the subtidal and intertidal regions and is likely a reflection of reduced tidal current competence deeper into the lagoon.

4. Discussion

4.1. Foraminiferal and taphonomic trends

Sediment inputs for Sur Lagoon predominantly come from three ephemeral wadis that occasionally flood during the rainy season, but do not provide a constant source of sediment. Wadi Shamah in particular, with its bird's foot delta, is likely one of the main inputs of new sediment into the lagoon (Figs. 2–3). Sediment is transported in and out of the lagoon via storms and tidal currents, with sediment removed from the Shallow Marine Area due to longshore transport or export to the steeply sloping shelf. The coastline to the NW and SE of Sur is very rocky with one large wadi to the NW of Sur that is also a potential sediment source.

The transport of sediment in and out of the lagoon, with residence time in both areas, is supported by foraminiferal results. Overall, there is not a large difference in the foraminiferal biofacies or taphofacies between the Shallow Marine Area and the Lagoon Basins (Main and Distal), even though there is considerable environmental difference with tidal exposure and wave climate inside and outside of the lagoon. The greatest difference is between the Distal Lagoon Basin and Shallow Marine Area, with the Main Lagoon Basin acting as a transitional zone (Figs. 6, 8–9; Tables 1–2). This similarity suggests that sediment spends residence time inside and outside of the lagoon inheriting taphonomic characteristics from both environments.

The abundance of miliolids, *A. tepida, A. parkinsoniana* and *E. gerthi* suggests they are the dominant taxa living in the lagoon, which is consistent with other similar coastal environments (e.g. Murray, 1991; Debenay et al., 2001; Lézine et al., 2002; Ghosh et al., 2009). The less-calcified specimens (e.g. *A. tepida*) are likely destroyed quickly in the Shallow Marine Area if exported from the lagoon, while the heavily calcified and larger *Amphistegina* spp. make their way into the Main Lagoon through storms (e.g. storm surge without the high rainfall of Gonu), but not into the Distal Lagoon Basin (Fig. 8). This is supported by particle size data showing a slight fining trend into the distal areas, and fossil fragment size which gets smaller into the Distal Lagoon (Figs. 3, 7, 9). Likewise, the abundance of fossil specimens is greatest in the Shallow Marine Area likely due to their robustness and resistance to fragmentation and abrasion in the more energetic wave-dominated regime (i.e. vs. the recent specimens; Tables 1–2; Fig. 9). Fossil specimens are likely eroding out of Tertiary rocks outcropping on the coast and shelf areas as there is not an increased abundance of them in the wadi channels.

The degree of corrasion also shows some relationship with distance into the lagoon but it is only expressed in the fossil foraminifera. Maximal corrasion is highest in the Main and Distal Lagoon Basins but this may be a size effect. The inner confines of the lagoon have higher quantities of fossil fragments which may have been exposed to corrasion for a longer period vs. whole fossils which are found in the outer marine areas (Fig. 9).

Corrasion with recent specimens did not show a predictable trend; it was present, but was highly variable within the basins (Table 2). The lack of a clear trend may be due to transport as discussed, or may relate to our ability to distinguish between dissolution and abrasion which would be correspondingly high inside vs. outside the lagoon.

4.2. Foraminiferal taphonomy as a potential overwash indicator

Based on the transect data, the most useful parameters for assessing an overwash event in Sur Lagoon will be the foraminifera taxa rather than the taphonomic characters per se (Figs. 8–9). The most useful taxa for recognizing a marine incursion (e.g. tsunami or storm) will be the abundance of *Amphistegina* spp., *A. inflata, E. advenum* and planktics, and these are expected to be highly concentrated through transport and sorting in an event bed. These species have higher r^2 values with distance into the lagoon, and a distinct transition from the Shallow Marine Area to the Main and Distal Lagoon Basins. Taphonomically, large specimen sizes (>250 μm) and high proportions of fossil specimens were also closely associated with the Shallow Marine Area and therefore may be useful as a potential overwash indicator. Of note is the presence of planktic taxa and large sized specimens, which have been used previously (e.g. Hawkes et al., 2007) with respect to the 2004 Indian Ocean tsunami, and based on this study will also prove important here.

5. Conclusions

In this arid intertidal lagoon at Sur, full taphonomic analysis is of limited value as the different environments are not causing a significant taphonomic imprint on the foraminifera. By far the most useful character is the foraminiferal assemblage itself and the enumeration of the number of fossil specimens. An overwash event at Sur Lagoon is expected to contain poorly sorted, heterogenous sand with relatively high abundances of *A. inflata*, *Amphistegina* spp., *E. advenum* and planktics, as well as large specimen sizes (>250 μm) and high proportions of fossil specimens. The best location to detect the overwash beds with foraminifera will be in the inner areas of the lagoon (Distal Lagoon and parts of the Main Lagoon Basins) where the number of robust specimens (recent or fossil) is low or non-existent. This study illustrates the need for baseline taphonomic data to determine the best target areas for finding overwash records in the stratigraphic record and to assess taphonomic overprinting that may occur during an extreme event (e.g. tsunami fragmentation of bivalves).

Supplementary materials related to this article can be found online at doi:10.1016/j.marmicro.2011.06.001.

Acknowledgments

The authors gratefully acknowledge (1) Richard Rothaus for field support, (2) Tom Vosmer and Barry Jupp for their assistance while on site in Oman, (3) Martin Knyf for technical assistance in McMaster's biogeochemistry laboratory, and (4) St. Cloud State University for the use of their Lowrance SONAR and Trimble R3. Funding was provided by NSERC research grants to Eduard Reinhardt (Discovery) and Jessica Pilarczyk (CGSM). This manuscript was greatly improved by comments from Ron Martin and two anonymous reviewers.

Appendix A

A.1. Systematics of Foraminifera

Faunal reference list for dominant taxa. The classification follows that of Hottinger et al. (1993), Hayward et al. (2004) and Loeblich and Tappan (1987). Systematics of individual species are from Hottinger et al. (1993) and references therein.

Amphistegina lessonii D'ORBIGNY, 1826
Amphistegina lobifera LARSEN, 1976
Ammonia inflata = *Rosalina inflata* SEGUENZA, 1862
Ammonia parkinsoniana = *Rosalina parkinsoniana* D'ORBIGNY, 1839
Ammonia tepida = *Rotalia beccarii var. tepida* CUSHMAN, 1936
Cibicides pseudolobatulus PERELIS & REISS, 1976
Elphidium advenum CUSHMAN, 1930
Elphidium craticulatum = *Nautilus craticulatus* FICHTEL & MOLL, 1798
Elphidium gerthi VAN VOORTHUYSEN, 1957
Elphidium striatopunctatum = *Nautilus striatopunctatus* FICHTEL & MOLL, 1798
Peneroplis planatus = *Nautilus planatus* FICHTEL & MOLL, 1798
Porosononion granosa = *Noionina granosa* D'ORBIGNY, 1846

References

Ambraseys, N.N., Melville, C.P., 1982. A History of Persian Earthquakes. Cambridge University Press, Cambridge. 219 pp.

Berkeley, A., Perry, C.T., Smithers, S.G., 2009. Taphonomic signatures and patterns of test degradation on tropical, intertidal benthic foraminifera. Mar. Micropaleontol. 73, 148–163.

Best, M.M.R., Kidwell, S.M., 2000. Bivalve taphonomy in tropical mixed siliciclastic-carbonate settings: environmental variation in shell condition. Paleobiology 26, 80–102.

Bhalla, S.N., Khare, N., Shanmukha, D.H., Henriques, P.J., 2007. Foraminiferal studies in nearshore regions of western coast of India and Laccadives Islands: a review. Indian J. Mar. Sci. 36, 272–287.

Bickert, T., Mackensen, A., 2004. Last glacial Holocene changes in South Atlantic deep water circulation. In: Wefer, G., Mulitza, S., Ratmeyer, V. (Eds.), The South Atlantic in the Late Quaternary: Reconstruction of Material Budgets and Current Systems. Springer-Verlag, pp. 671–695.

Chandler, G.T., Williams, D.F., Spero, H.J., Xiaodong, G., 1996. Sediment microhabitat effects on carbon stable isotopic signatures of microcosm-cultured benthic foraminifera. Limnol. Oceanogr. 41, 680–688.

Cherif, O.H., Al-Ghadban, A., Al-Rifaiy, I.A., 1997. Distribution of foraminifera in the Arabian Gulf. Micropaleontology 43, 253–280.

Culver, S.J., Woo, H.J., Oertel, G.F., Buzas, M.A., 1996. Foraminifera of coastal depositional environments, Virginia, U.S.A.: distribution and taphonomy. Palaios 11, 459–486.

Debenay, J.-P., Geslin, E., Eichler, B.B., Duleba, W., Sylvestre, F., Eichler, P., 2001. Foraminiferal assemblages in a hypersaline lagoon, Araruama (R. J.) Brazil. J. Foramineferal Res. 31, 133–151.

De Francesco, C.G., Hassan, G.S., 2008. Dominance of reworked fossil shells in modern estuarine environments: implications for paleoenvironmental reconstructions based on biological remains. Palaios 23, 14–23.

Deil, U., 1996. Zur Kenntnis der Adiantetea-Gesellschaften des Mittelmeerraumes und umliegender Gebiete. Phytocoenologia 26, 481–536.

Donato, S.V., Reinhardt, E.G., Boyce, J.I., Pilarczyk, J.E., Jupp, B.P., 2009. Particle-size distribution of inferred tsunami deposits in Sur Lagoon, Sultanate of Oman. Mar. Geol. 257, 54–64.

Donato, S.V., Reinhardt, E.G., Boyce, J.I., Rothaus, R., Vosmer, T., 2008. Identifying tsunami deposits using bivalve shell taphonomy. Geology 36, 199–202.

El-Nakhal, H., 1990. Geographical distribution of the foraminiferal genus *Agglutinella*. Micropaleontology 36, 86–87.

Fishbein, E., Patterson, R.T., 1993. Error-weighted maximum likelihood (EWML): a new statistically based method to cluster quantitative micropaleontological data. J. Paleontol. 67, 475–486.

Fritz, H.M., Blount, C.D., Albusaidi, F.B., Al-Harthy, A.H.M., 2010. Cyclone Gonu storm surge in Oman. Estuarine Coastal Shelf Sci. 86, 102–106.

Ghosh, A., Saha, S., Saraswati, P.K., Banerjee, S., Burley, S., 2009. Intertidal foraminifera in the macro-tidal estuaries of the Gulf of Cambay: implications for interpreting sea-level change in palaeo-estuaries. Mar. Pet. Geol. 26, 1592–1599.

Hawkes, A.D., Bird, M., Cowie, S., Grundy-Warr, C., Horton, B.P., Tan Shau Hwai, A., Law, L., Macgregor, C., Nott, J., Eong Ong, J., Rigg, J., Robinson, R., Tan-Mullins, M., Tiong, T., Yasin, Z., Wan Aik, L., 2007. Sediments deposited by the 2004 Indian Ocean tsunami along the Malaysia–Thailand Peninsula. Mar. Geol. 242, 169–190.

Hayward, B.W., Holzmann, M., Grenfell, H.R., Pawlowski, J., Triggs, C.M., 2004. Morphological distinction of molecular types in *Ammonia* — towards a taxonomic revision of the world's most commonly misidentified foraminifera. Mar. Micropaleontol. 50, 237–271.

Heidarzadeh, M., Pirooz, M.D., Zaker, N.H., Yalciner, A.C., Mokhtari, M., Esmaeily, A., 2008. Historical tsunami in the Makran Subduction Zone off the southern coasts of Iran and Pakistan and results of numerical modeling. Ocean Eng. 35, 774–786.

Hippensteel, S.P., Martin, R.E., 1999. Foraminifera as an indicator of overwash deposits, Barrier Island sediment supply, and Barrier Island evolution: Folly Island, South Carolina. Palaeogeogr. Palaeoclimatol. Palaeoecol. 149, 115–125.

Hippensteel, S.P., Martin, R.E., 2000. Foraminifera of storm-generated washover fans: implications for determining storm frequency in relation to sediment supply and barrier island evolution, Folly Island, South Carolina. In: Martin, R.E. (Ed.), Environmental Micropaleontology: Topics in Geobiology. Kluwer Academic/Plenum Publication, New York, pp. 351–369.

Hippensteel, S.P., Martin, R.E., Harris, M.S., 2005. Records of prehistoric hurricanes on the South Carolina coast based on micropaleontological and sedimentological evidence, with comparison to other Atlantic Coast records: discussion. Geol. Soc. Am. Bull. 117, 250–253.

Hippensteel, S.P., Martin, R.E., Nikitina, D., Pizzuto, J.E., 2000. The formation of Holocene marsh foraminiferal assemblages, middle Atlantic Coast, U.S.A.: implications for Holocene sea-level change. J. Foramineferal Res. 30, 272–293.

Hottinger, L., Halicz, E., Reiss, Z., 1993. Recent foraminifera from the Gulf of Aqaba, Red Sea. Slovenska Akademija Znanosti in Umenosti (Ljubljana), classis IV, dela, 33, 179, 230 pp.

Kortekaas, S., Dawson, A.G., 2007. Distinguishing tsunami and storm deposits: an example from Martinhal, SW Portugal. Sediment. Geol. 200, 208–221.

Lézine, A., Saliège, J., Mathieu, R., Tagliatela, T., Mery, S., Charpentier, V., Cleuziou, S., 2002. Mangroves of Oman during the late Holocene: climatic implications and impact on human settlements. Veg. Hist. Archaeobot. 11, 221–232.

Loeblich, A.R., Tappan, H., 1987. Foraminiferal Genera and their Classification. Van Nostrand Rienhold Co., New York.

Luque, L., Lario, J., Civis, J., Silva, P.G., Zazo, C., Goy, J.L., Dabrio, C.J., 2002. Sedimentary record of a tsunami during Roman times, Bay of Cadiz, Spain. J. Quaternary Sci. 17, 623–631.

Mackensen, A., Rudolph, M., Kuhn, G., 2001. Late Pleistocene deepwater circulation in the subantarctic eastern Atlantic. Glob. Planet. Change 30, 197–229.

Mamo, B., Strotz, L., Dominey-Howes, D., 2009. Tsunami sediments and their foraminiferal assemblages. Earth Sci. Rev. 96, 263–278.

Martin, R.E., 1999. Taphonomy: A Process Approach. Cambridge University Press, Cambridge. 508 pp.

Martin, R.E., Harris, M.S., Liddell, W.D., 1995. Taphonomy and time-averaging of foraminiferal assemblages in Holocene tidal flat sediments, Bahia La Choya, Sonora, Mexico (Northern Gulf of California). Mar. Micropaleontol. 26, 187–206.

Martin, R.E., Wehmiller, J.F., Harris, M.S., Liddell, W.D., 1996. Comparative taphonomy of bivalves and foraminifera from Holocene tidal flat sediments, Bahia la Choya, Sonora, Mexico (Northern Gulf of California): taphonomic grades and temporal resolution. Paleobiology 22, 80–90.

Moghaddasi, B., Nabavi, S.M.B., Vosoughi, G., Fatemi, S.M.R., Jamili, S., 2008. Abundance and distribution of benthic foraminifera in the Northern Oman Sea (Iranian Side) continental shelf sediments. Res. J. Environ. Sci. 3, 210–217.

Murray, J.W., 1965. The foraminiferida of the Persian Gulf. 2. The Abu Dhabi region. Palaeogeogr. Palaeoclimatol. Palaeoecol. 1, 307–332.

Murray, J.W., 1966a. The foraminiferida of the Persian Gulf. 3. The Halat Al Bahrani region. Palaeogeogr. Palaeoclimatol. Palaeoecol. 2, 59–68.

Murray, J.W., 1966b. The foraminiferida of the Persian Gulf. 4. Khor Al Bazam. Palaeogeogr. Palaeoclimatol. Palaeoecol. 2, 153–169.

Murray, J.W., 1966c. The foraminiferida of the Persian Gulf. 5. The shelf off the Trucial Coast. Palaeogeogr. Palaeoclimatol. Palaeoecol. 2, 267–278.

Murray, J.W., 1991. Ecology and Paleoecology of Benthic Foraminifera. John Wiley & Sons, Inc. 397p.

Murray, J.W., Alve, E., 1999. Taphonomic experiments on marginal marine foraminiferal assemblages: how much ecological information is preserved? Palaeogeogr. Palaeoclimatol. Palaeoecol. 149, 183–197.

Murray, M.R., 2002. Is laser particle size determination possible for carbonate-rich lake sediments? J. Paleolimnol. 27, 173–183.

Nigam, R., Khare, N., 1995. Recent foraminifera along west coast of India: retrospect, perspect and prospect. J. Indian Acad. Geosci. 38, 7–24.

Okal, E.A., Synolakis, C.E., 2008. Far-field tsunami hazard from mega-thrust earthquakes in the Indian Ocean. Geophys. J. Int. 172, 995–1015.

Parsons-Hubbard, K.M., 2005. Molluscan taphofacies in recent carbonate reef/lagoon systems and their application to sub-fossil samples from reef cores. Palaios 20, 175–191.

Patterson, R.T., Fishbein, E., 1989. Re-examination of the statistical methods used to determine the number of point counts needed for micropaleontological quantitative research. J. Paleontolog. 63, 245–248.

Patterson, R.T., Kumar, A., 2000. Use of arcellacea to gauge levels of pollution and remediation of industrially polluted lakes. In: Martin, R.E. (Ed.), Environmental Micropaleontology, v. 15 of Topics in Geobiology. Kluwer Academic/Plenum Publication, New York, pp. 257–278.

Patterson, R.T., Kumar, A., 2002. A review of current testate rhizopod (thecamoebian) research in Canada. Palaeogeogr. Palaeoclimatol. Palaeoecol. 180, 225–251.

Peebles, M.W., Lewis, R.D., 1991. Surface textures of benthic foraminifera from San-Salvador, Bahamas. J. Foramineferal Res. 21, 285–292.

Peros, M.C., Reinhardt, E.G., Davis, A.M., 2007. High-resolution paleosalinity reconstruction from Laguna de la Leche, north coastal Cuba, using Sr, O, and C isotopes. Palaeogeogr. Palaeoclimatol. Palaeoecol. 245, 535–550.

Pilarczyk, J.E., Reinhardt, E.G., 2011. *Homotrema rubrum* (Lamarck) taphonomy as an overwash indicator in marine ponds on Anegada, British Virgin Islands. Nat. Hazards. doi:10.1007/s11069-010-9706-3.

Reddy, K.R., Rao, R.J., 1984. Foraminifera-salinity relationship in the Pennar Estuary, India. J. Foramineferal. Res. 14, 115–119.

Reinhardt, E.G., Goodman, B.E., Boyce, J.I., Lopez, G., van Hengstum, P., Rink, W., Mart, Y., Raban, A., 2006. The Tsunami of December 13, 115 A.D. and the destruction of Herod the Great's Harbor at Caesarea Maritima, Israel. Geology 34, 1061–1064.

Sambridge, M., Braun, J., McQueen, H., 1995. Geophysical parametrization and interpolation of irregular data using natural neighbors. Geophys. J. Int. 122, 837–857.

Schils, T., Wilson, S.C., 2006. Temperature threshold as a biogeographic barrier in northern Indian Ocean macroalgae. J. Phycol. doi:10.1111/j.1529-8817.2006.00242.x.

Scott, D.B., Collins, E.S., Gayes, P.T., Wright, E., 2003. Records of prehistoric hurricanes on the South Carolina coast based on micropaleontological and sedimentological evidence, with comparison to other Atlantic Coast records. Geol. Soc. Am. Bull. 115, 1027–1039.

Sultan, S.A.R., Elghribi, N.M., 1996. Temperature inversion in the Arabian Gulf and the Gulf of Oman. Cont. Shelf Res. 16, 1521–1544.

Szuman, M., Berndt, C., Jacobs, C., Best, A., 2006. Seabed characterization through a range of high-resolution acoustic systems — a case study offshore Oman. Mar. Geophys. Res. 27, 167–180.

van Hengstum, P.J., Reinhardt, E.G., Boyce, J.I., Clark, C., 2007. Changing sedimentation patterns due to historical land-use change in Frenchman's Bay, Pickering, Canada: evidence from high-resolution textural analysis. J. Paleolimnol. 37, 603–618.